Photothermal Amplification of Cu-Porphyrin Redox Chemistry on Ti_3C_2 MXene for NIR-Activated Reactive Oxygen Species Generation for the Treatment of Hepatocellular Carcinoma

Ushmita Dey, Antara Ghosh, Nilanjan Das, Archana Singh, Sumanta Kumar Sahu*

Department of Chemistry and Chemical Biology, Indian Institute of Technology (ISM), Dhanbad 826004, Jharkhand, India

*Corresponding author. E-mail: sksahu@iitism.ac.in, sumantchem@gmail.com

Fax: +91 326-2307772; Tel: +91 3262235936

---

1. Experimental Section

1.1 Synthesis of TCPP and Cu-TCPP

1.1.1 Synthesis of TPPCOOMe

First, 6.83 g of methyl-4-formylbenzoate (41.6 mmol) was added to a 250 mL round-bottom (RB) flask containing 100 mL of propionic acid. The RB was covered in aluminium foil to ensure dark conditions. The mixture was stirred for a few minutes using a magnetic stirrer until the solid was completely dissolved. Next, 2.80 mL of freshly distilled pyrrole (40.4 mmol) was added dropwise to the mixture while stirring. The solution was then heated to 150 °C for 12 hours in the dark under reflux conditions. The reaction mixture was cooled down to room temperature, and the purple product was collected by vacuum filtration. Warm de-ionised water, methanol, and ethyl ether were used sequentially to remove impurities. The product was dried at 50 °C in a vacuum oven, and the yield was calculated to be 20%.

1.1.2 Synthesis of TCPP

0.846 g of TPPCOOMe (1 mmol) was dissolved in a 50 ml 1:1 (by volume) solution of THF and Methanol. 2.8 g of KOH (50 mmol) was dissolved in 25 mL of DI water to make a 2 M solution, which was then carefully added to the previous solution. The mixture was stirred at 80 °C under reflux conditions for 12 hours. Once the reaction mixture had cooled to room temperature, the volatile part was removed using a rotary evaporator. Next, a 1M HCl solution was used to acidify the mixture to pH 3. The resulting precipitate was separated using vacuum filtration and then washed with an excess of water. The purple product was dried in a vacuum oven at 50 °C, and the yield was calculated to be 90%.

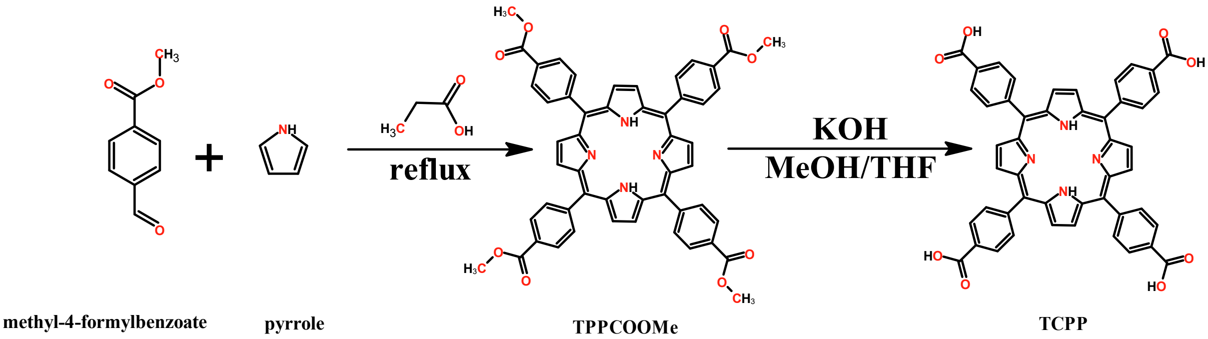

Figure S1 Synthesis scheme for TCPP

1.1.3 Synthesis of Cu-TPPCOOMe

0.846 g of TPPCOOMe (1 mmol) was dissolved in 100 mL of DMF. Next, 2.2 g of CuCl2 · 2H2O (12.8 mmol) was added to the solution. The mixture was stirred at 160 °C under reflux conditions for 6 hours. Once the reaction mixture had cooled to room temperature, it was diluted with 150 mL of water. The precipitate was collected by vacuum filtration and washed with a copious amount of DI water. The solid was dissolved in $CHCl_3$ and extracted with DI water 3 times. The organic layer was passed through anhydrous sodium sulphate and evaporated to get a red powder as the product. Yield was 70%.

1.1.4 Synthesis of Cu-TCPP

The obtained Cu-TPPCOOMe was dissolved in a 50 mL 1:1 (v/v) solution of THF and Methanol. 2.8 g of KOH (50 mmol) was dissolved in 25 mL of DI water to make a 2 M solution and added carefully to the previous solution. The mixture was stirred at 80 °C under reflux conditions for 12 hours. Once the reaction mixture had cooled to room temperature, the volatile part was removed using a rotary evaporator. Next, a 1M HCl solution was used to acidify the mixture to pH 3. The resulting red coloured precipitate was separated using vacuum filtration and washed with water. The product was dried in a vacuum oven at 50 °C, and the yield was calculated to be 90%.

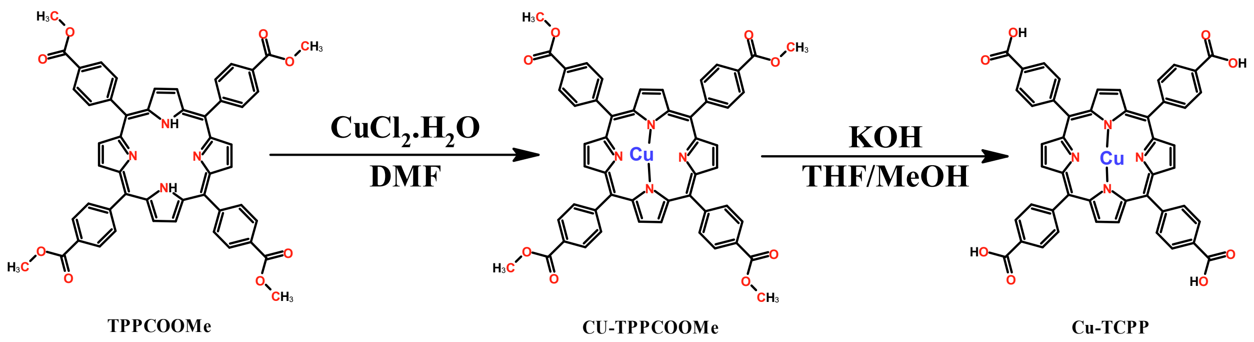

Figure S2 Synthesis scheme for Cu-TCPP

1.2 Calculation of Photothermal conversion efficiency (η)

The photothermal conversion efficiency (η) of the Ti_3C_2@UCNP@Cu-TCPP@LA was calculated according to the established Roper method using the heating-cooling temperature profiles. Briefly, an aqueous dispersion of Ti_3C_2@UCNP@Cu-TCPP@LA was irradiated with an 808 nm laser at a constant power density (1 W Cm^{-2}) until a steady-state maximum temperature (T_{max}) was reached. The laser was then switched off, and the subsequent cooling process was recorded. Four successive heating-cooling cycles were conducted to evaluate photothermal stability. Pure water served as a control under identical experimental conditions.

The photothermal conversion efficiency (η) was calculated using the following equation,

$$\eta = \frac{hS(T_{max} - T_{surr}) - Q_{dis}}{I(1 - 10^{-A_{808}})}$$

In this equation, h is the heat transfer coefficient, and S is the surface area of the container. T_{max} is the maximum steady-state temperature of the solution, and T_{surr} is the ambient temperature. Q_{dis} is the heat dissipation from the light absorption by the quartz cuvette and solvent (determined using pure water), I is the laser power, and A_{808} is the absorbance of the aqueous dispersion of the Ti_3C_2@UCNP@Cu-TCPP@LA at the irradiation wavelength 808 nm.

The heat transfer coefficient (hS) was obtained by fitting the cooling curve according to the following equation,

$$\theta = \frac{T - T_{Surr}}{T_{Max} - T_{Surr}}$$

The time constant (τ_s) of the system was determined from the linear fitting of $-\ln(\theta)$ vs time during the cooling process, as expressed by,

$$-\ln(\theta) = \frac{t}{\tau_s}$$

Subsequently, hS was calculated using the following equation,

$$hs = \frac{m_D C_D}{\tau_s}$$

where m_D and C_D denote the mass and specific heat capacity of the solvent (water), respectively.Under 808 nm laser irradiation (1 W cm^{-2}), the temperature of Ti_3C_2@UCNP@Cu-TCPP@LA aqueous dispersion increased from 24.5 °C to 46.9 °C. The system time constant (τ_s) obtained from the cooling curve was 176.25 s. In addition, m_D is 0.3 g and C_D is 4.2 J/g.°C. So, the calculated value of hS is 0.0059 W/°C. The calculated value of Q_{dis} is 0.031 W, and the absorbance of Ti_3C_2@UCNP@Cu-TCPP@LA at 808 nm was 0.11, and the resulting photothermal conversion efficiency (η) was calculated to be 57.16%.

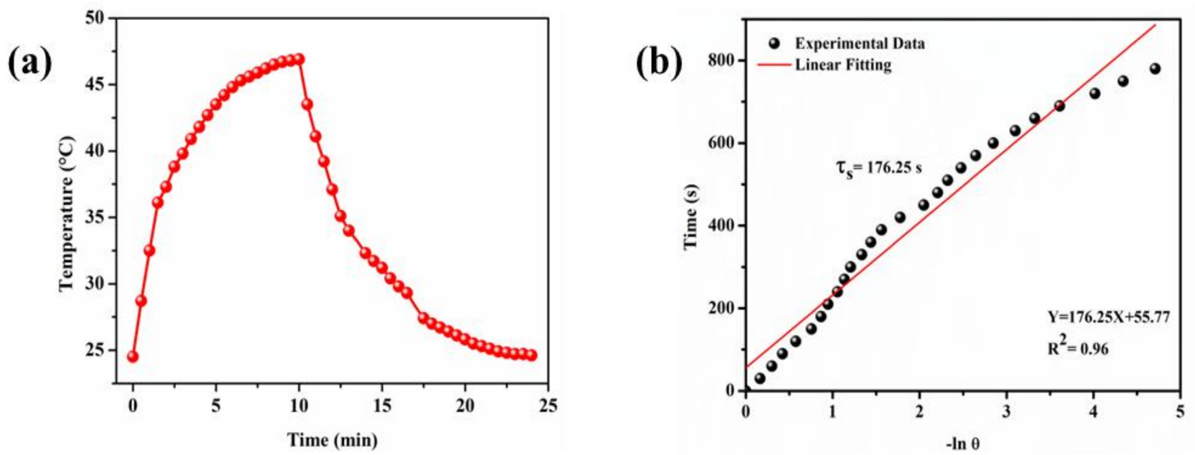

Figure S3 (a) Heating-cooling curve of Ti_3C_2@UCNP@Cu-TCPP@LA, (b) linear plot of time vs -ln(θ) for calculation of photothermal conversion efficiency of Ti_3C_2@UCNP@Cu-TCPP@LA

2. ^{1}H NMR spectra

(a)

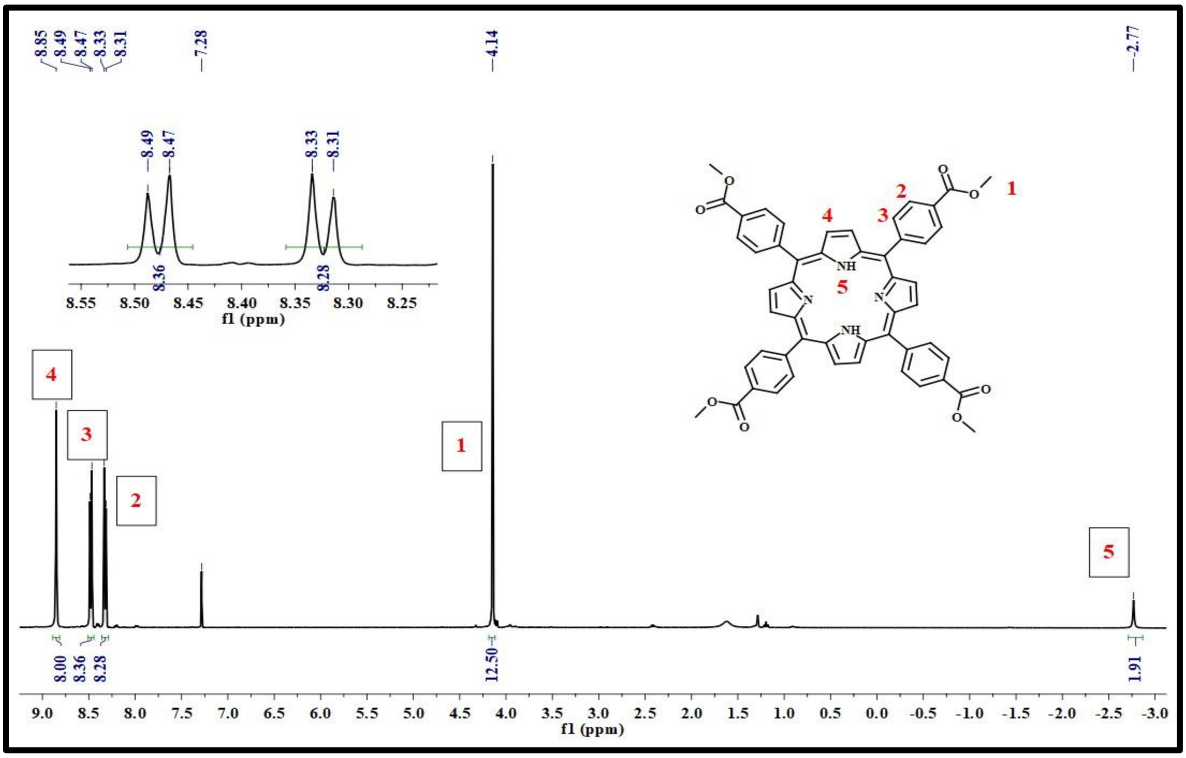

^{1}H NMR (400 MHz, $CDCl_3$, ppm): δ =8.85 (s, 8H), 8.48 (d, 8H), 8.32 (d, 8H), 4.14 (s, 12H), -2.77 (s, 2H).

(b)

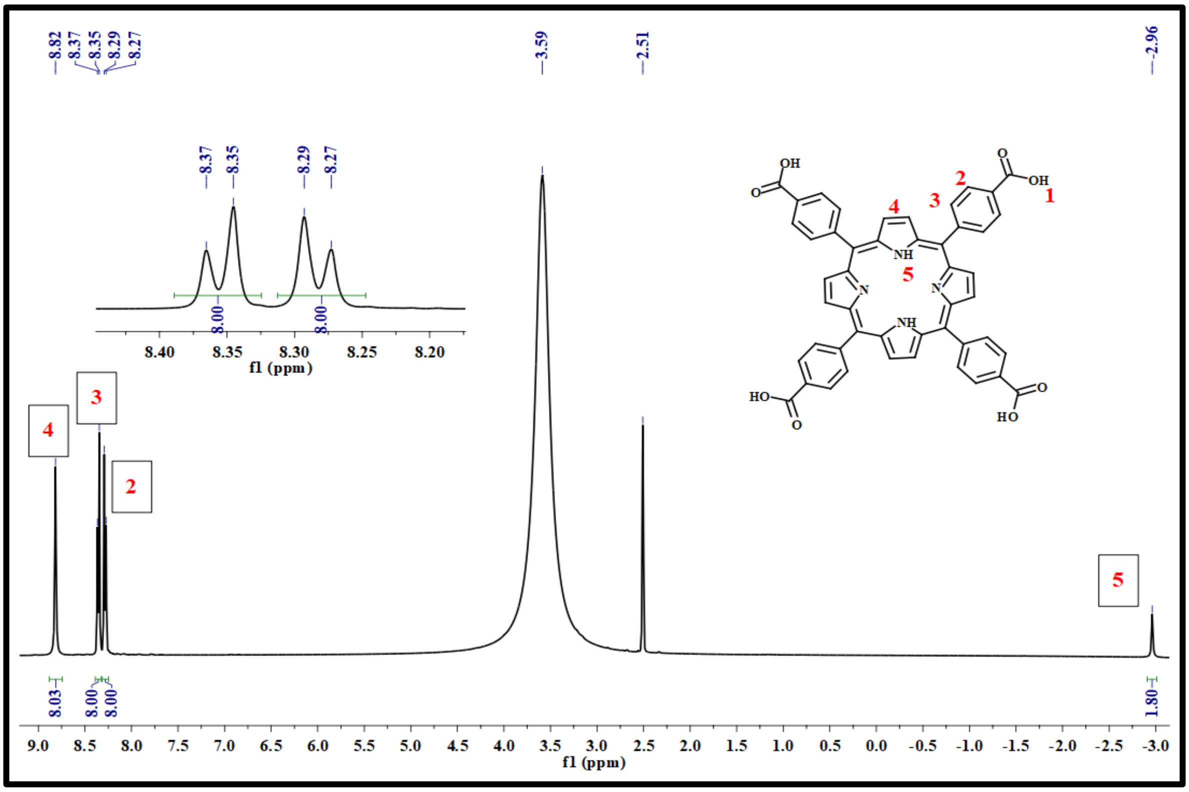

^{1}H NMR (400 MHz, DMSO-d6, ppm): δ =8.82 (s, 8H), 8.36 (d, 8H), 8.28 (d, 8H), -2.96 (s, 2H).

Figure S4 ^{1}H NMR Spectra of (a) TPPCOOMe and (b) TCPP

3. High-resolution mass spectra

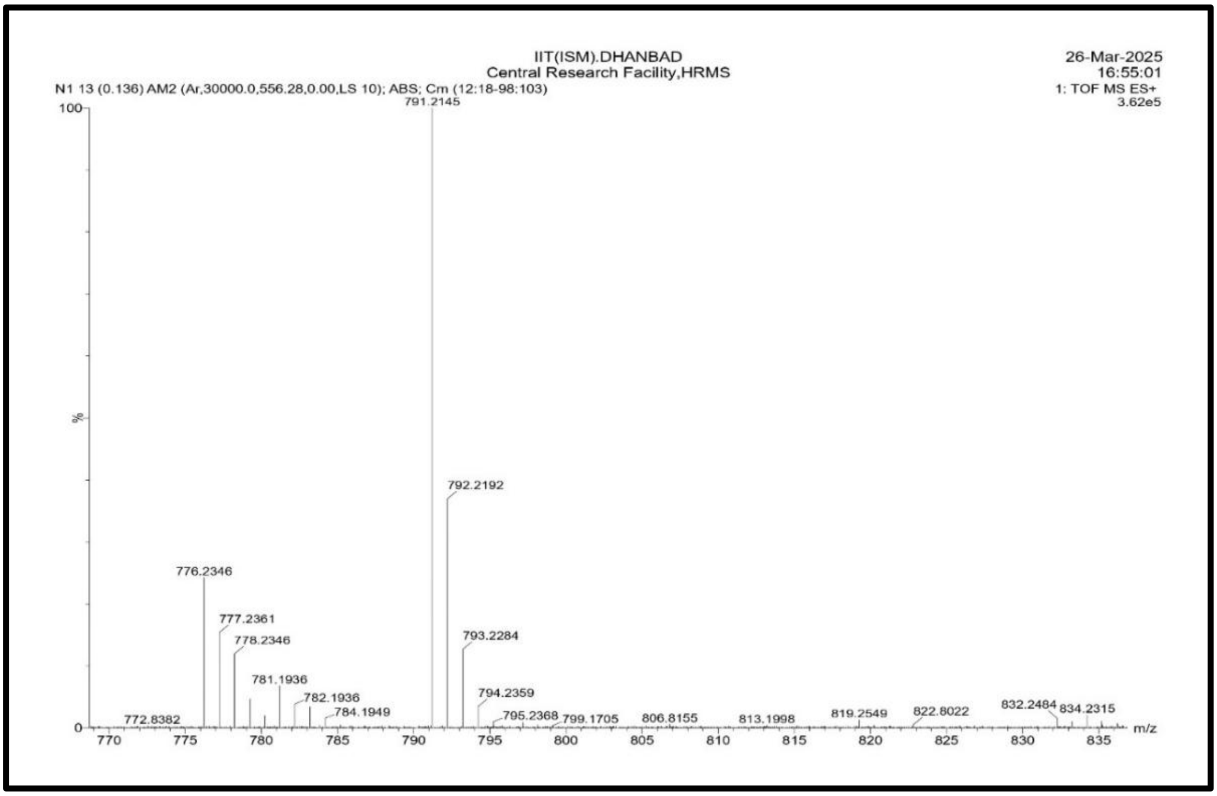

MALDI-TOF: m/z 791.2 ($[MH]^+$) ($C_{48}H_{30}N_4O_8$)

Figure S5 HRMS of TCPP

4. HRTEM images and SAED pattern

4.1. SAED and lattice pattern of Ti_3C_2 and UCNP

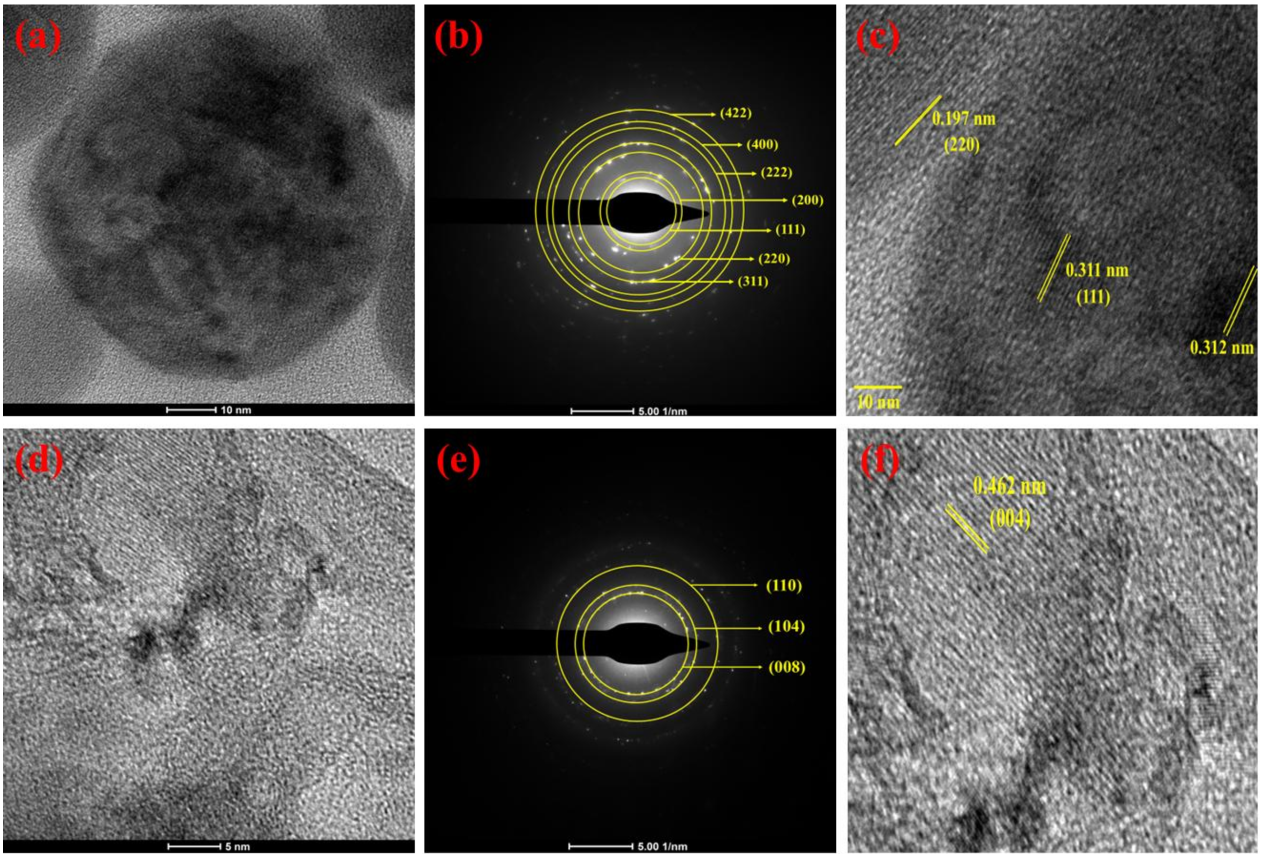

Figure S6 (a, c) HRTEM images of NaYF4:Yb,Er,Nd (UCNP), (b) SAED pattern of UCNP, (d, f) HRTEM images of Ti_3C_2, (b) SAED pattern of Ti_3C_2

4.2. SAED and lattice pattern of Ti_3C_2@UCNP

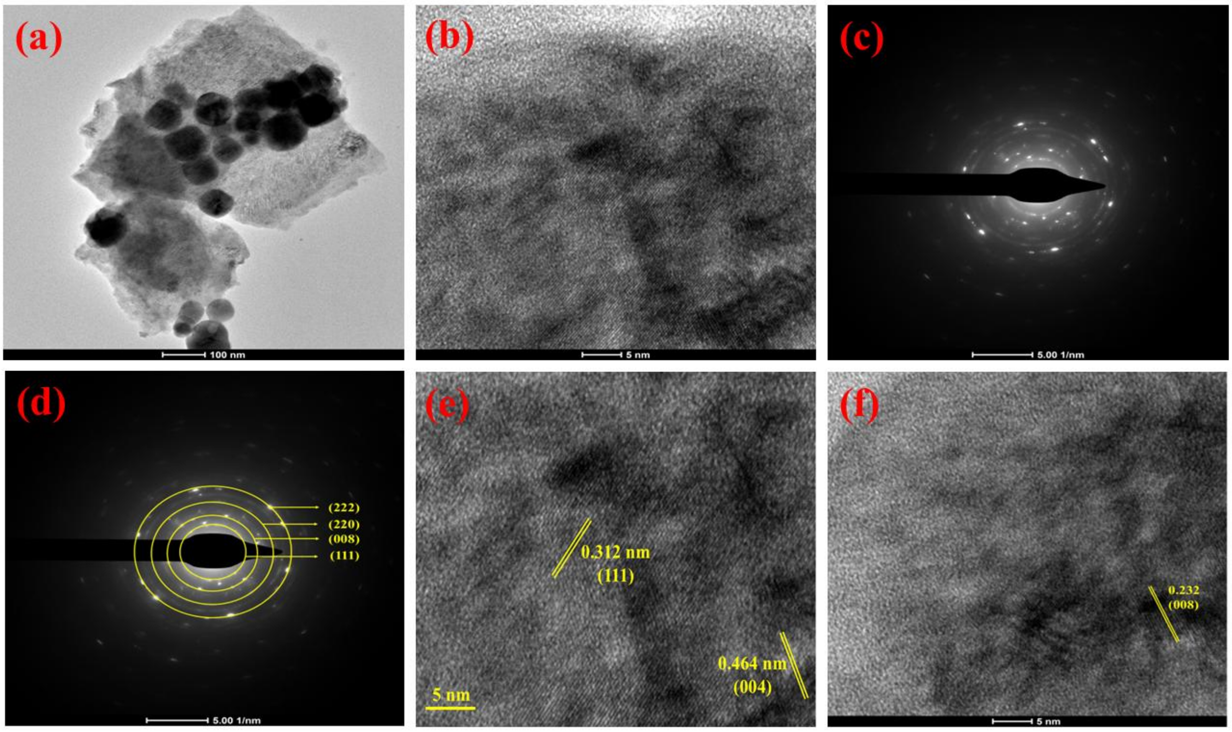

Figure S7 (a,b,e,f) HRTEM images of Ti_3C_2@UCNP, (c,d) SAED pattern of Ti_3C_2@UCNP

5. EDAX analysis

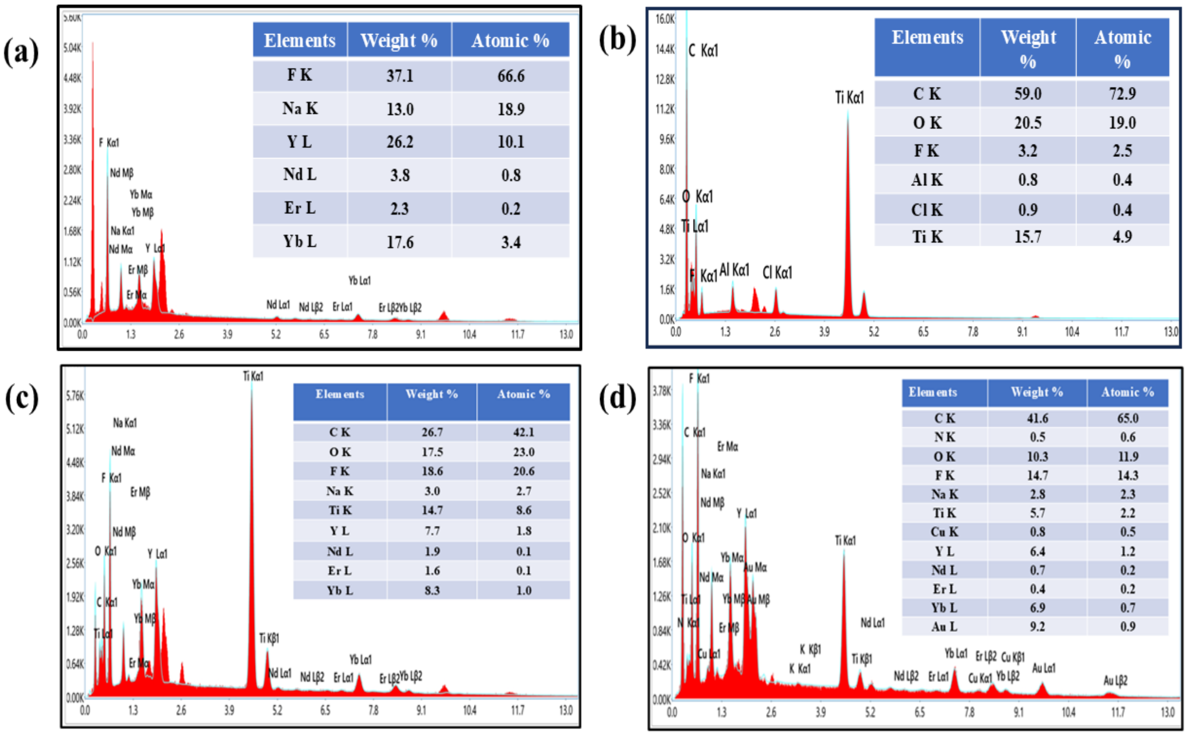

Figure S8 EDAX Spectra and elemental composition of (a) $NaYF_4$: Yb, Er, Nd (UCNP), (b) Ti_3C_2, (c) Ti_3C_2@UCNP and (d) Ti_3C_2@UCNP@Cu-TCPP

6. FESEM images

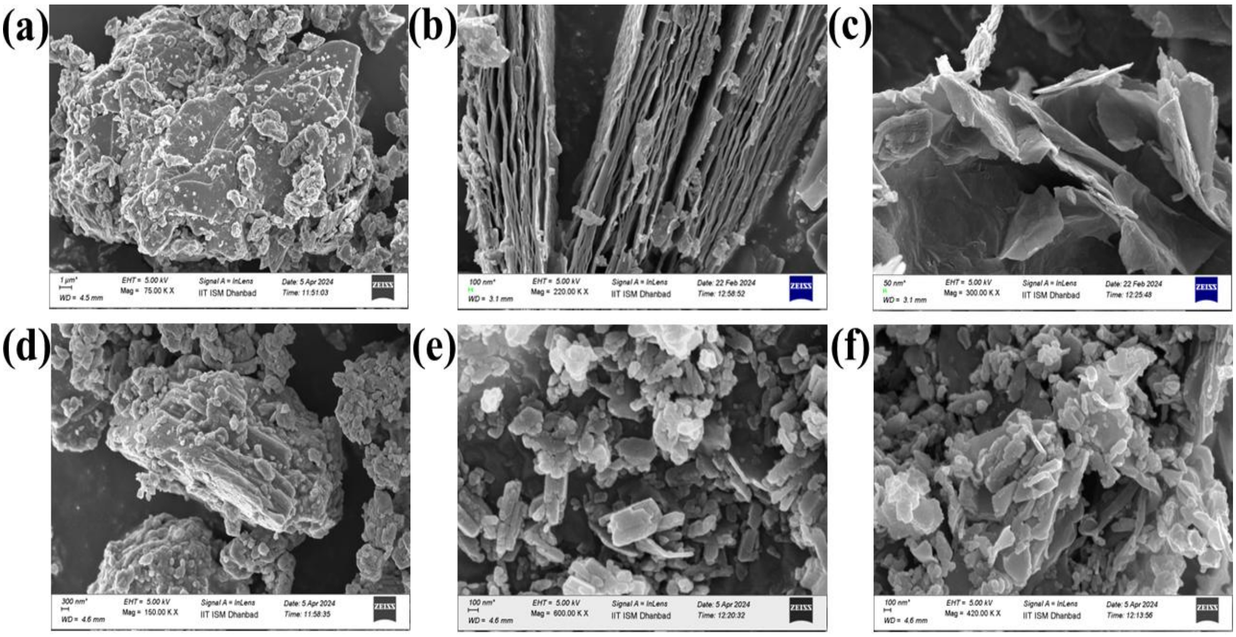

Figure S9 FESEM images of (a) nonmilled MAX phase (Ti_3AlC_2), (b) MXene (Ti_3C_2) and (c) Delaminated MXene synthesised from non-milled MAX phase, (d) Ball-milled MAX phase (Ti_3AlC_2), (e,f) Delaminated MXene synthesised from ball-milled MAX phase

7. FTIR Spectra

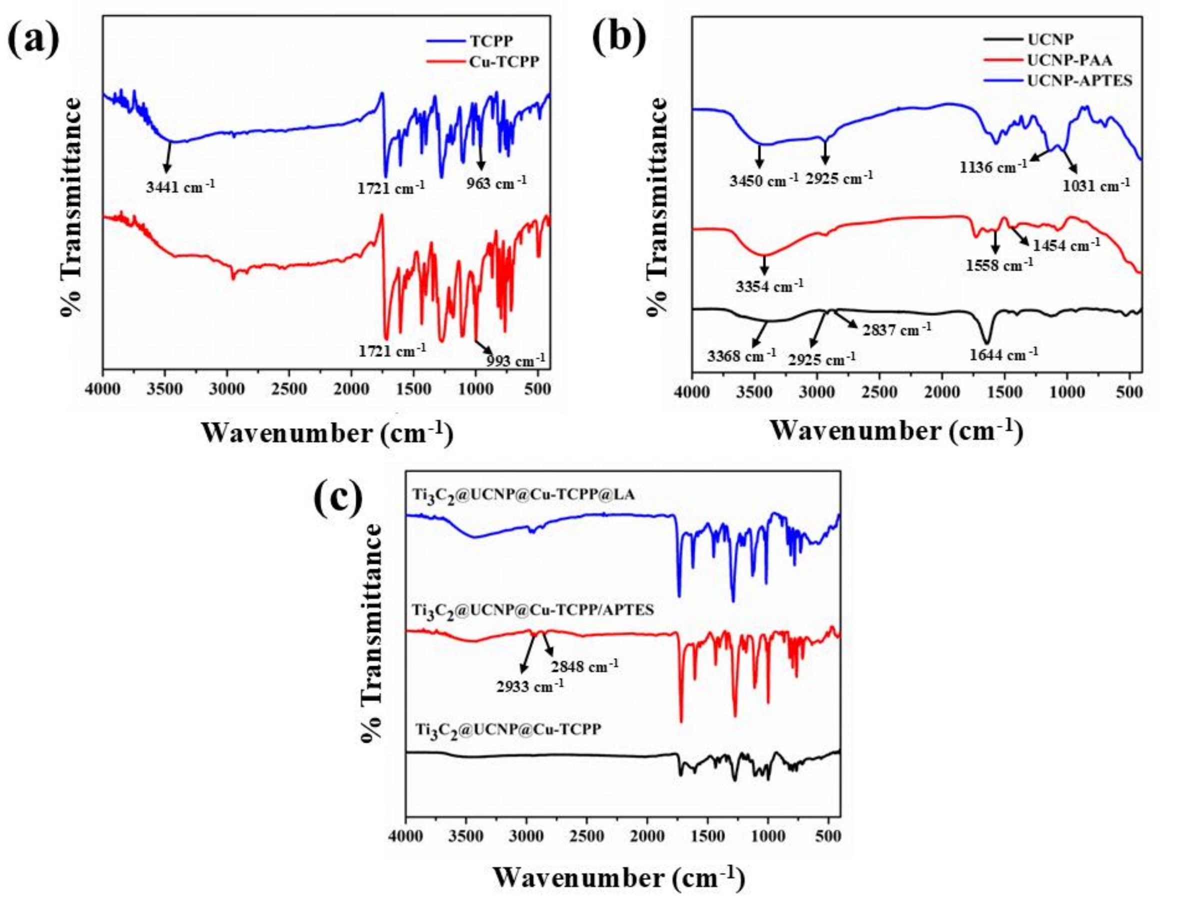

Figure S10 FTIR spectra of (a) TCPP and Cu-TCPP, (b) UCNP, UCNP-PAA and UCNP-PAA-APTES, (c) Ti_3C_2@UCNP@Cu-TCPP, Ti_3C_2@UCNP@Cu-TCPP/APTES, and Ti_3C_2@UCNP@Cu-TCPP@LA

8. XRD Spectra

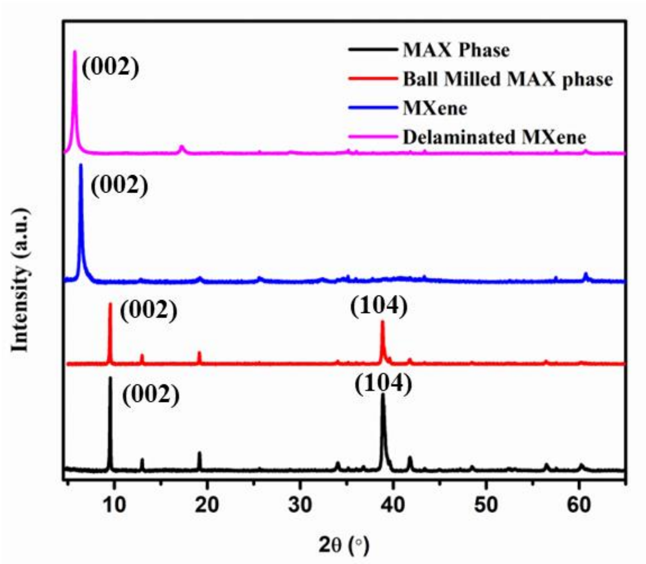

Figure S11 XRD spectra of MAX phase (Ti_3AlC_2), Ball milled MAX Phase (Ti_3AlC_2), MXene (Ti_3C_2) and Delaminated MXene (Ti_3C_2)

9. High-resolution XPS Spectra

9.1. XPS spectra of TCPP and Cu-TCPP

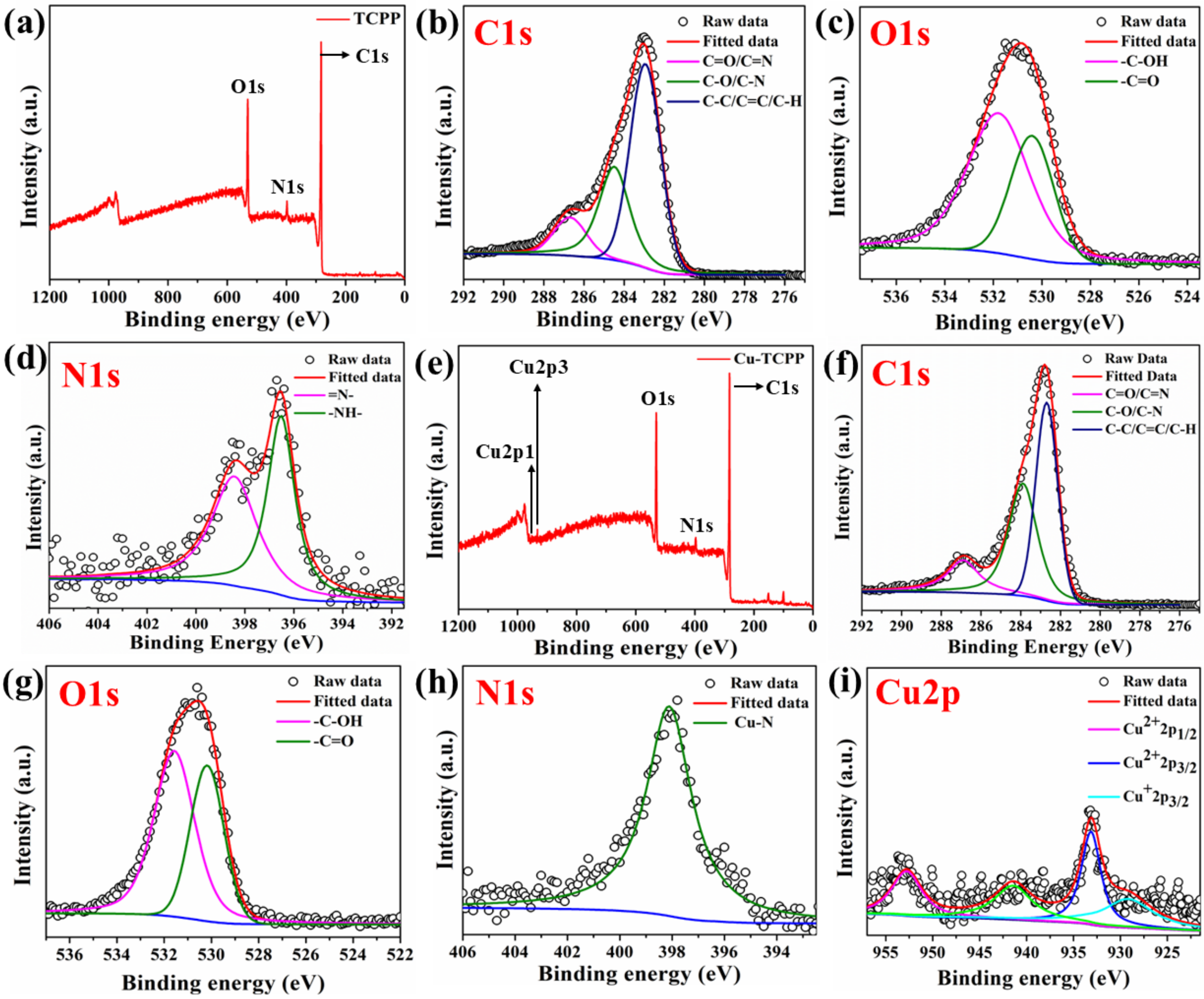

Figure S12 Elemental survey spectra of (a) TCPP and (e) Cu-TCPP, (b-d) Deconvolution spectra of C1s, O1s, N1s for TCPP and (f-i) Deconvolution spectra of C1s, O1s, N1s and Cu2p for Cu-TCPP

9.2. XPS spectra of UCNP, Ti_3C_2 and UCNP@Ti_3C_2

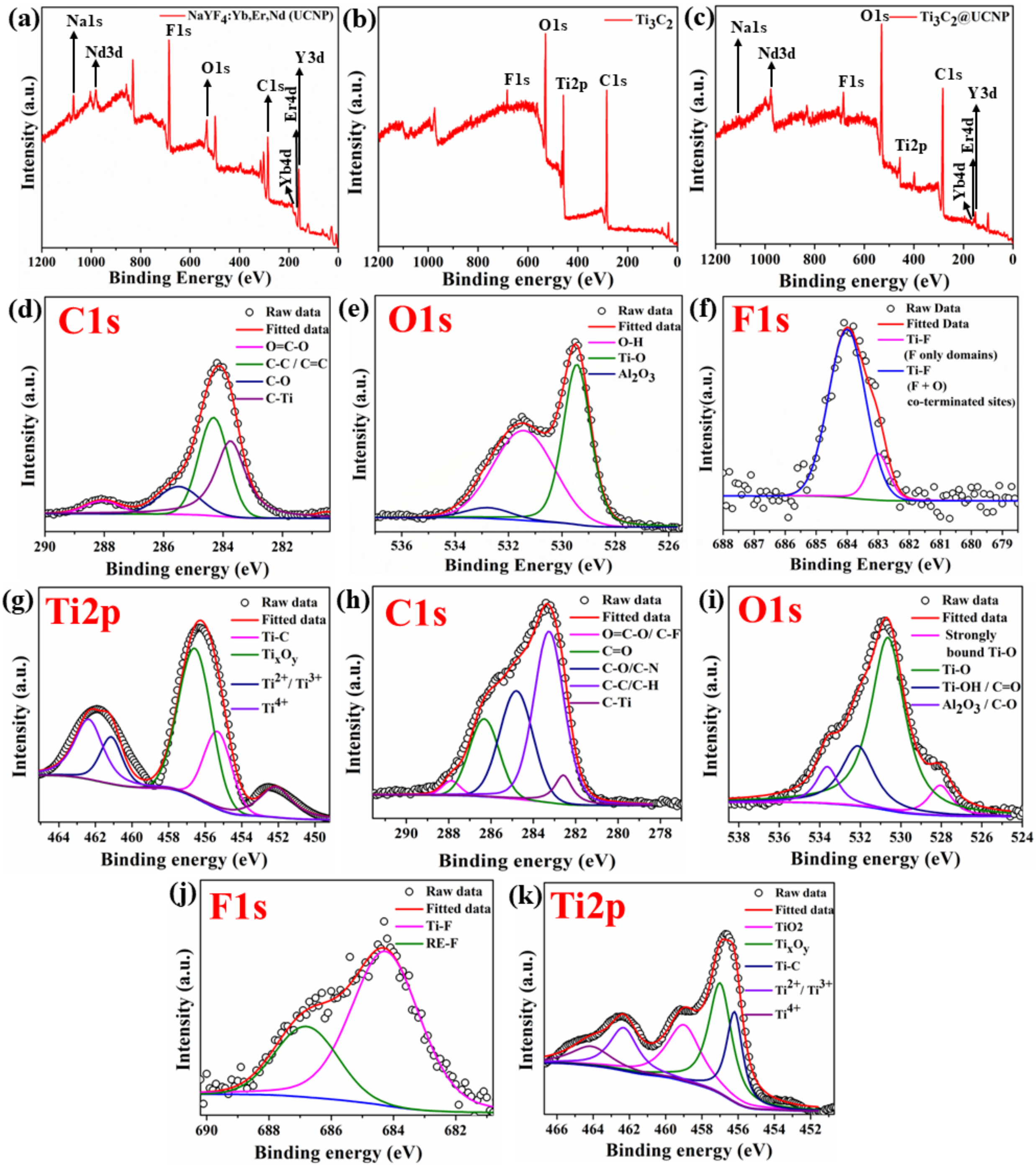

Figure S13 Elemental survey spectra of (a) $NaYF_4$:Yb,Er,Nd (UCNP), (b) Ti_3C_2 and (c) Ti_3C_2@UCNP, (d-g) Deconvolution spectra of C1s, O1s, N1s, Ti2p for Ti_3C_2 and (h-k) Deconvolution spectra of C1s, O1s, N1s and Ti2p for Ti_3C_2@UCNP

9.3 XPS spectra of Ti_3C_2@UCNP@Cu-TCPP

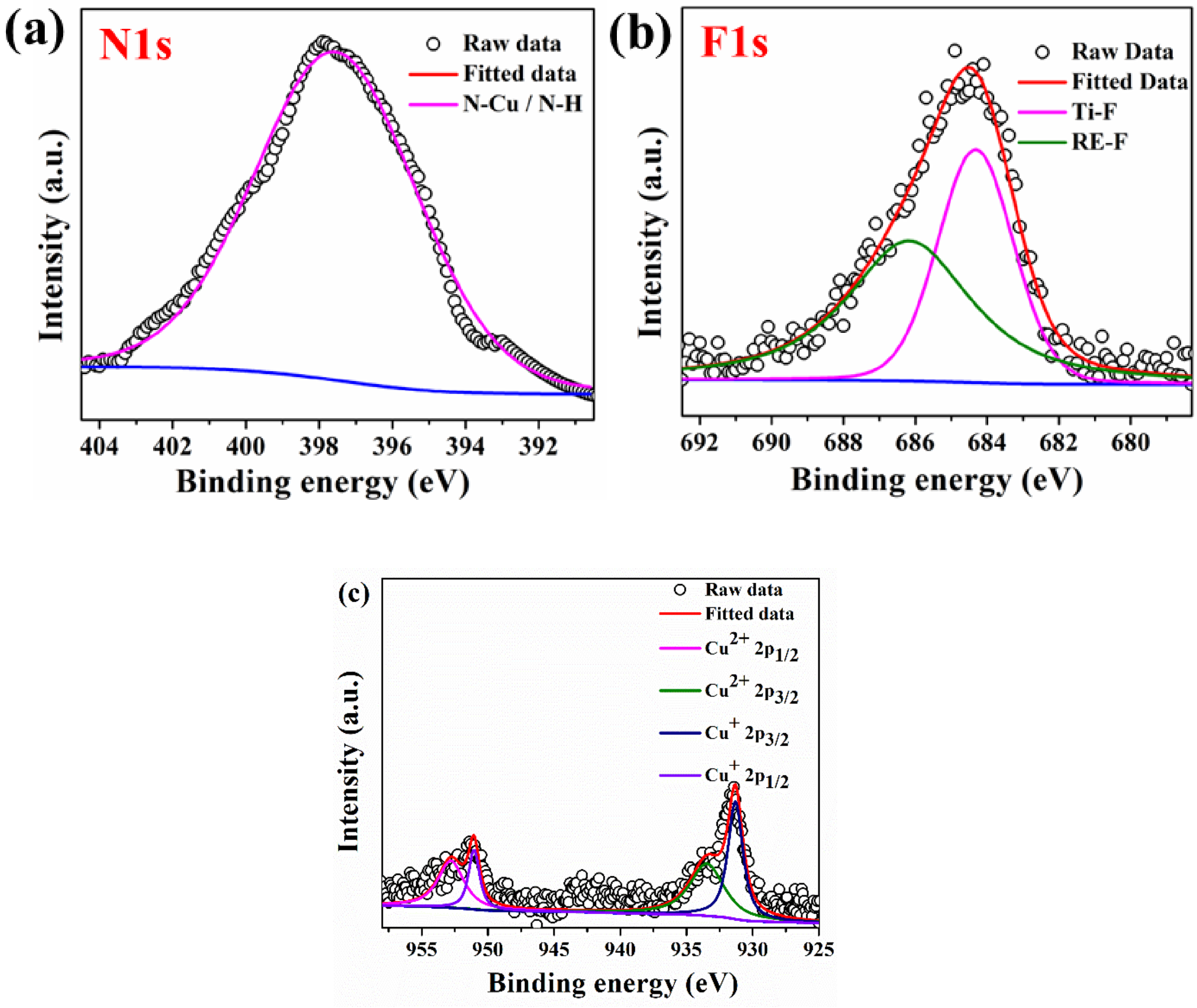

Figure S14 Deconvolution spectra of (a) N1s, (b)F1s and (c) Cu2p incubated with GSH for Ti_3C_2@UCNP@Cu-TCPP

10. Photographic Images

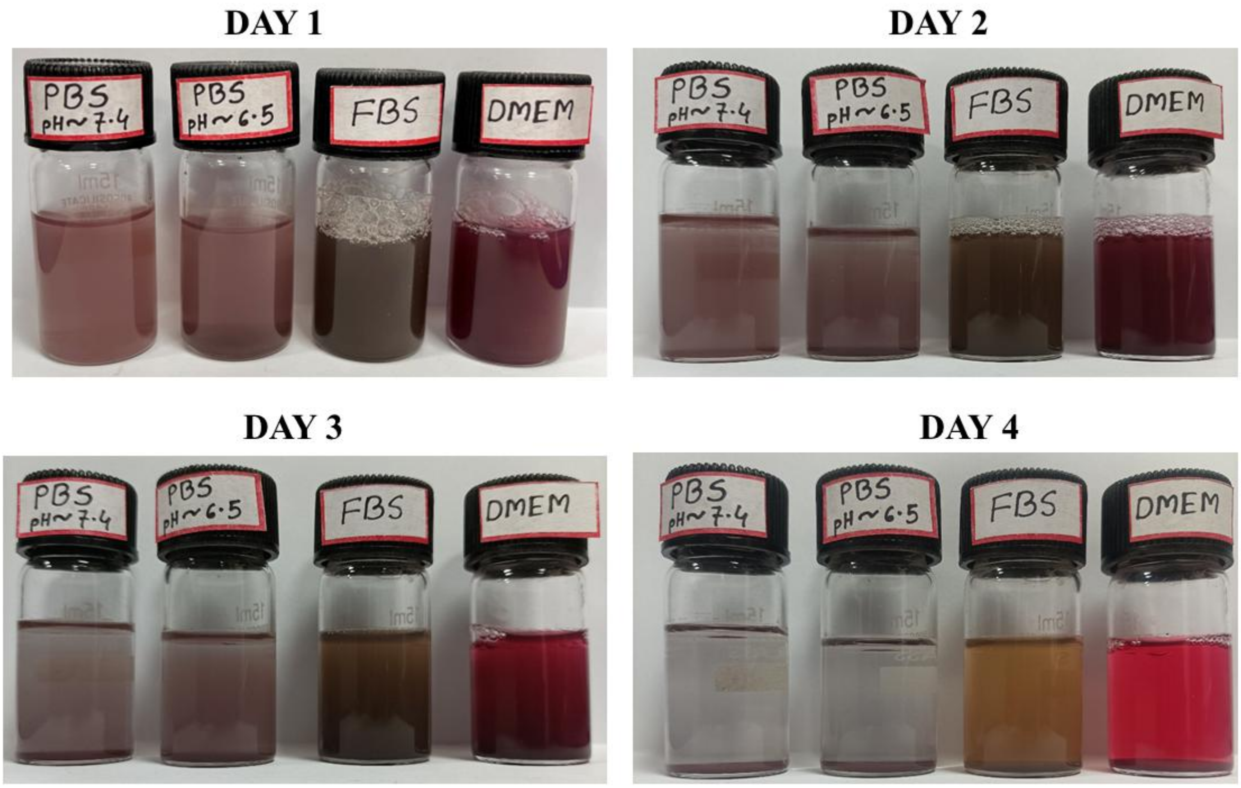

Figure S15 Stability of Ti_3C_2@UCNP@Cu-TCPP@LA in lysosomal pH (PBS, pH 7.4) and cancer cell pH (PBS, pH 6.5), FBS and DMEM medium over a duration of 4 days.

11. DTNB absorption spectra and ICP-OES study

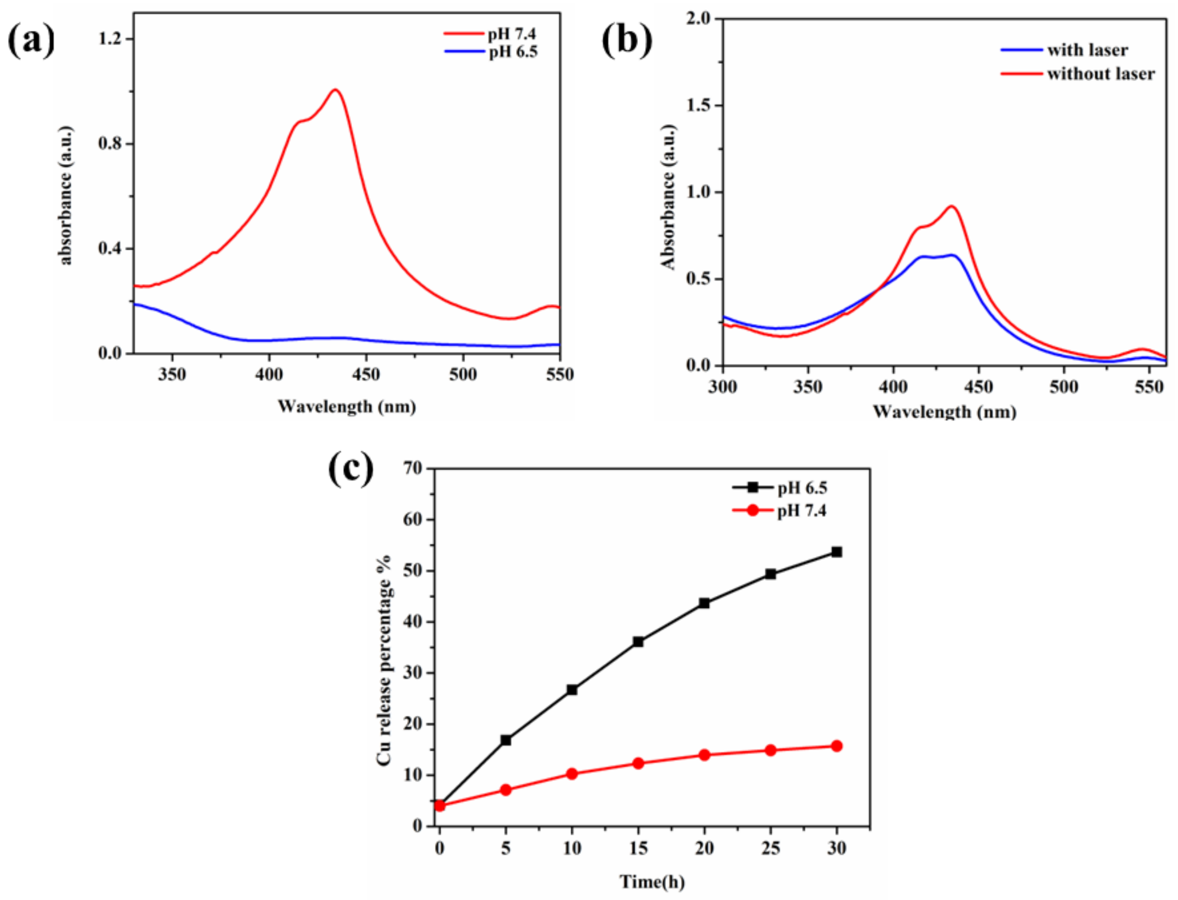

Figure S16 (a) Absorption spectra of DTNB with variation in pH, (b) Absorption spectra of DTNB with laser and without laser, (c) ICP-OES study for the percentage of Cu release under lysosomal pH and cancer cell pH

12. MTT Assay

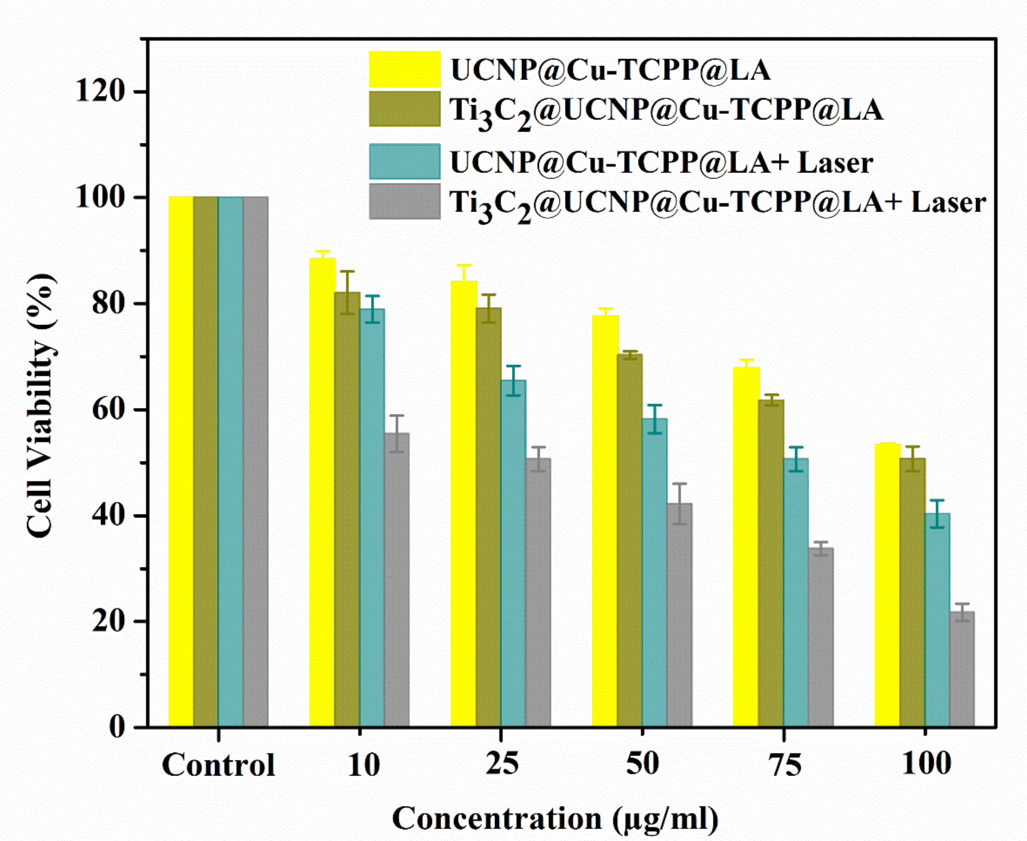

Figure S17 Comparative Cytotoxicity or MTT assay of UCNP@Cu-TCPP@LA, Ti_3C_2@UCNP@Cu-TCPP@LA, UCNP@Cu-TCPP@LA + Laser and Ti_3C_2@UCNP@Cu-TCPP@LA + Laser in the HepG2 cell line.

13. Cellular Uptake Study

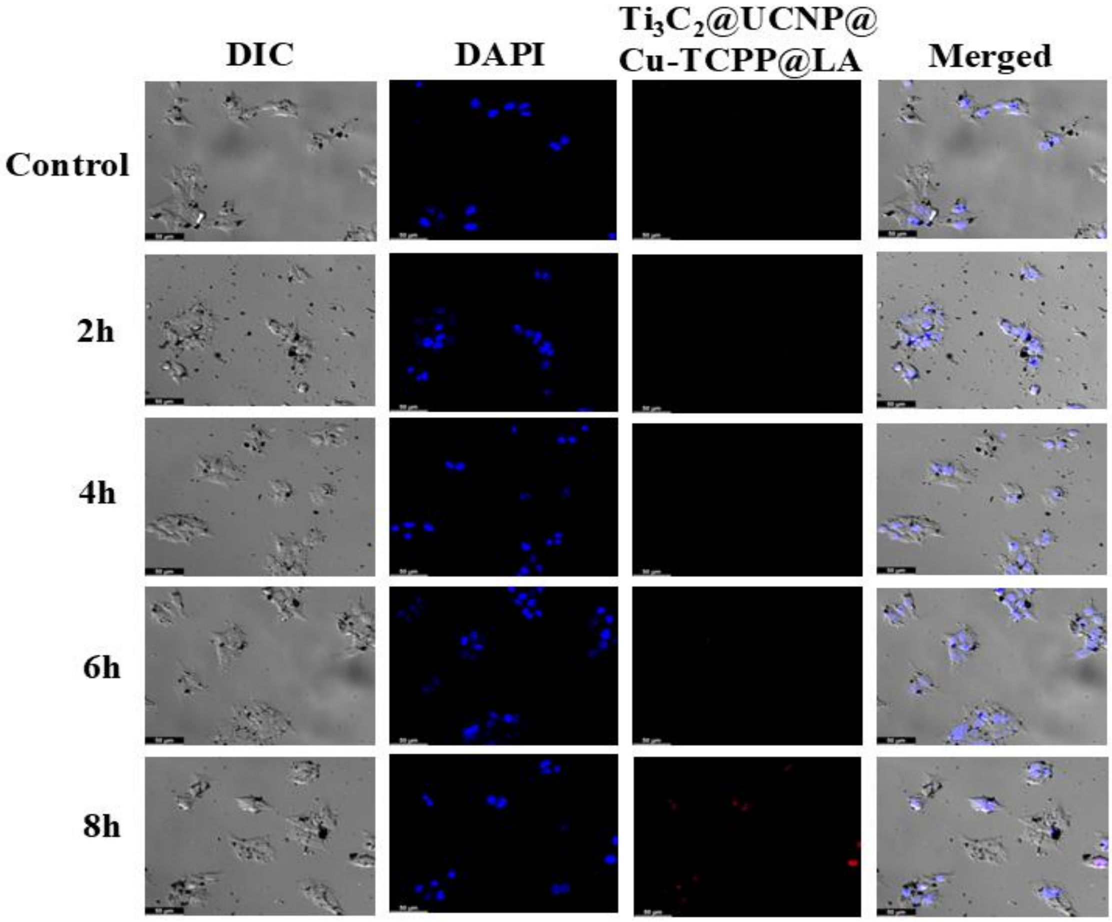

Figure S18 Cellular uptake study of Ti_3C_2@UCNP@Cu-TCPP@LA in HEK293 cells over 8h